J|A|C|S
ARTICLES
Published on Web 08/30/2006

Hydration and Dewetting near Fluorinated Superhydrophobic Plates

Xin Li,[†] Jingyuan Li,[‡] Maria Eleftheriou,[§] and Ruhong Zhou*[,†,§]

Contribution from the Department of Chemistry, Columbia University, New York, New York 10027, Department of Physics, Zhejiang University, Hangzhou, China, and IBM Thomas J. Watson Research Center, Yorktown Heights, New York 10598

Received December 8, 2005; E-mail: ruhongz@us.ibm.com

Abstract: The water dynamics near nanoscale fluorinated ($CF_3(CF_2)_7(CH_2)_2SiH_3$) monolayers (plates) as well as possible dewetting transitions in-between two such plates have been studied with molecular dynamics simulations in this paper. A "weak water depletion" is found near the single fluorinated surface, with an average water density in the first solvation shells 6−8% lower than its hydrogenated counterpart. The fluorinated molecules are also found to be water impermeable, consistent with experimental findings. More surprisingly, a dewetting transition is found in the interplate region with a critical distance D_c of 10 Å (3−4 water diameters) for double plates with 8 × 8 molecules each (plate size ≈ 4 nm × 4 nm). This transition, although occurring on a microscopic length scale, is reminiscent of a first-order phase transition from liquid to vapor. The unusual superhydrophobicity of fluorocarbons is found to be related to their larger size (or surface area) as compared to hydrocarbons, which "dilutes" their physical interactions with water. The water−plate interaction profile shows that the fluorinated carbons have a 10−12% weaker water−plate interaction than their hydrogenated counterparts in the nearest solvation shell, even though the fluorocarbons do have a stronger electrostatic interaction with water due to their larger partial charges. However, the van der Waals interactions dominate the water−plate interaction within the nearest shell, with up to 90% contributions to the total interaction energy, and fluorocarbons have a noticeably weaker (by 10−15%) van der Waals interaction with water in the nearest shell than do hydrocarbons. Both the slightly weaker water−plate interaction and larger surface area contribute to the stronger dewetting transition in the current fluorinated carbon plates.

1. Introduction

Hydrophobic effects play a key role in many important physio-chemical processes, such as micelle formation,[1] water permeation in membrane channels (aquaporins),[2,3] subcellular self-assembly,[4] and superhydrophobic surface coating.[5] Concurrent with the progress on experimental work,[5−9] there has been a growing interest in theoretical studies of complex and more realistic systems with strong hydrophobicity.[10−12] In contrast to small solutes that can fit into the water hydrogen-bond network, larger hydrophobic solutes or surfaces can induce reorganization of water molecules such as drying or dewetting layers.[1,13−18] Many groups such as the Chandler group have studied this important phenomena using both computer simulations and analytical theories.[19−35] A dewetting transition has

[†] Columbia University.
[‡] Zhejiang University.
[§] IBM Thomas J. Watson Research Center.

(1) Hummer, G.; Garde, S.; Garcia, A. E.; Pratt, L. R. *Chem. Phys.* **2000**, *258*, 349−370.
(2) Beckstein, O.; Biggin, P. C.; Sansom, M. S. P. *J. Phys. Chem. B* **2001**, *105*, 12902−12905.
(3) Beckstein, O.; Sansom, M. S. P. *Proc. Natl. Acad. Sci. U.S.A.* **2003**, *100*, 7063−7068.
(4) Brooks, C. L.; Gruebele, M.; Onuchic, J. N.; Wolynes, P. G. *Proc. Natl. Acad. Sci. U.S.A.* **1998**, *95*, 11037.
(5) Erbil, H. Y.; Demirel, A. L.; Avci, Y; Mert, O. *Science* **2003**, *299*, 1377−1380.
(6) Steitz, R.; Gutberlet, T.; Hauss, T.; Klosgen, B.; Krastev, R.; Schemmel, S.; Simonsen, A. C.; Findenegg, G. H. *Langmuir* **2003**, *19*, 2409−2418.
(7) Jensen, T. R.; Jensen, M. O.; Reitzel, N.; Balashev, K.; Peters, G. H.; Kjaer, K.; Bjornholm, T. *Phys. Rev. Lett.* **2003**, *90*, 86101(1−4).
(8) Ball, P. *Nature* **2003**, *423*, 25−26.
(9) Genzer, J.; Efimenko, K. *Science* **2000**, *290*, 2130−2133.
(10) Cheng, Y.; Rossky, P. J. *Nature* **1998**, *392*, 696−699.
(11) Zhou, R.; Huang, X.; Margulius, C. J.; Berne, B. J. *Science* **2004**, *305*, 1605−1609.
(12) Liu, P.; Huang, X.; Zhou, R.; Berne, B. J. *Nature* **2005**, *437*, 159−162.
(13) Stillinger, F. H. *J. Solution Chem.* **1973**, *2*, 141.
(14) Wallqvist, A.; Gallicchio, E.; Levy, R. M. *J. Phys. Chem. B* **2001**, *105*, 6745−6753.
(15) Lum, K.; Luzar, A. *Phys. Rev. E* **1997**, *56*, 6283−6286.
(16) Chandler, D. *Nature* **2002**, *417*, 491.
(17) Ashbaugh, H. S.; Paulaitis, M. E. *J. Am. Chem. Soc.* **2001**, *123*, 10721−10728.
(18) Werder, T.; Walther, J. H.; Jaffe, R. L.; Halicioglu, T.; Koumoutsakos, P. *J. Phys. Chem. B* **2003**, *107*, 1345.
(19) Lum, K.; Chandler, D.; Weeks, J. D. *J. Phys. Chem. B* **1999**, *103*, 4570−4577.
(20) Huang, D. M.; Chandler, D. *J. Phys. Chem. B* **2002**, *106*, 2047−2053.
(21) Sansom, M. S. P.; Biggin, P. C. *Nature* **2001**, *414*, 156−159.
(22) Bérard, D. R.; Attard, P.; Patey, G. N. *J. Chem. Phys.* **1993**, *98*, 7236−7244.
(23) Paulaitis, M. E.; Pratt, L. R. *Adv. Protein Chem.* **2002**, *62*, 283−310.
(24) Bratko, D.; Curtis, R. A.; Blanch, H. W.; Prausnitz, J. M. *J. Chem. Phys.* **2001**, *115*, 3873−3877.
(25) Wallqvist, A.; Berne, B. J. *J. Phys. Chem.* **1995**, *99*, 2893−2899.
(26) Hummer, G.; Rasaiah, J. R.; Noworyta, J. P. *Nature* **2001**, *414*, 188−190.
(27) Leung, K.; Luzar, A.; Bratko, D. *Phys. Rev. Lett.* **2003**, *90*, 65502(1−4).
(28) Lee, C. Y.; McCammon, J. A.; Rossky, P. J. *J. Chem. Phys.* **1984**, *80*, 4448−4455.
(29) Huang, X.; Margulis, C. J.; Berne, B. J. *Proc. Natl. Acad. Sci. U.S.A.* **2003**, *100*, 11953−11958.
(30) Huang, X.; Zhou, R.; Berne, B. J. *J. Phys. Chem. B* **2005**, *109*, 3546−3552.

been observed in simple model systems,[19,25] graphite-like plates[30,33,35] (or carbon nanotubes[26]) with reduced carbon−water interaction, and paraffin-like plates.[30] The effect of an electric field on this dewetting transition has also been studied for graphite-like plates.[35] However, much less has been done with structurally and chemically more complex systems.[10,11,36]

It is now known from previous simulations[29,30,33,35] as well as macroscopic theory that the critical distance for drying between two hydrophobic plates will increase as the strength of the attractive interactions decreases. The critical distance will also increase as the plate sizes increase.[29,30] For example, no dewetting was found between two seemingly very hydrophobic domain interfaces in a multidomain protein BphC enzyme, but dewetting did occur when the attractive electrostatic and van der Waals interactions between the protein and water were turned off.[11] For hydrophobic paraffin-like plates with a size of a few nanometers, a dewetting transition with a small critical distance of about 7 Å (holding one layer of water molecules) was found,[30] while, on the other hand, a strong dewetting transition with a critical distance up to 14 Å was observed for idealized purely repulsive plates with a comparable size.[29]

Searching for superhydrophobic molecules is of current interest for many applications, ranging from submarine coating to novel water nanopore design.[2,3,37] The dewetting transition studies provide a unique way for better understanding the mechanism behind subcellular self-assemblies, as well as water nanopores and molecular on−off switches. Genzer and Efimenko have recently discovered a new family of molecules that display superhydrophobic surfaces in their mechanically assembled monolayers.[5,9] The common characteristic shared by these molecules is that they are all chain-like molecules with semi-fluorinated carbon groups. It has been previously found that fluorinated chains might possess a higher hydrophobicity than their hydrogenated counterparts. Some empirical rules have also been proposed, such as the $1CF_2 \approx 1.5CH_2$ rule, to semiquantitatively describe the relative hydrophobicity strength, based on experimental data such as free energy for ligand partitioning (between water and octanol) and ligand binding (i.e., one CF_2 group contributes about 1.5 times the partitioning or binding free energy as one CH_2 group).[38,39] In Genzer and Efimenko's work, it was found that the water contact angle with the mechanically assembled fluorocarbon monolayer can be higher than 135°. This high water contact angle and well-defined surface (as compared to many other superhydrophobic surfaces with complicated topologies from coating, etching, etc.[5]) might be an ideal case for our dewetting transition studies. It has been shown in our previous work[29,30] that the dewetting transition only happens when the water contact angle is larger than 90°, and the dewetting critical distance $D_c \propto \cos \theta_c$.[29] Thus, under normal conditions, there is no dewetting transition for graphite plates, because the water contact angle on the graphite surface is only about 86°.[40] The water contact angle for paraffin is estimated to be about 115°,[30] which gives a critical distance of about 7 Å for a comparable-sized plate.[30] For the current fluorinated superhydrophobic plates, a larger critical distance might be expected due to its larger water contact angle.

In this work, we devise a molecular system to mimic as closely as possible the experimental setup of Genzer and Efimenko,[9] but focus our study on water hydration and dewetting transitions, rather than water contact angles. We prepare two systems for computer modeling: one is a single superhydrophobic plate (surface) with fluorocarbons "anchored" on an 8×8 square lattice to mimic the silicon substrate attaching; and the other is a double-plate system, with each plate consisting of 8×8 molecules and their terminal $-CF_3$ groups facing each other. We then solvate the two model systems in explicit water to investigate the dynamical behavior of water molecules near the interfacial regions. We also made attempts to probe the underlying physical interactions governing the unusual superhydrophobicity of these fluorinated carbon systems. In doing so, we replace all of the fluorinated carbons with their hydrogenated counterparts and repeat all of the simulations. The results from both hydrogenated and fluorinated systems indicate that the stronger dewetting transition displayed by the latter is related to its larger surface area than that of the former. The physical interaction between fluorocarbons and water is also found to be about 10−12% weaker than that of the hydrocarbons in the nearest solvation shells, which contributed to the stronger dewetting as well. Fluorine is the most electronegative of all elements, and its dense electron cloud has very low polarizability.[39,41] This low polarizability and relatively larger size (as compared to hydrogen atom) result in weak van der Waals interactions of fluorocarbons with water, even weaker than hydrocarbons with water. Even though the electrostatic interactions between fluorinated carbons and water are indeed stronger than their hydrogenated counterparts due to their larger partial charges, the van der Waals interactions, nonetheless, are found to be the dominant force in the water−plate interactions.

This paper will be organized as follows. In section 2, we describe the molecular systems and simulation methods used. Section 3 presents the simulation results and the in-depth analysis, with emphasis on the dewetting transition inside the double plates. Finally, section 4 provides the conclusion and outlines the future direction.

2. System and Methods

In the present study, as an effort to mimic the system built by Genzer and Efimenko in their pioneering experimental work,[9] a layer of fluorinated carbons made of 64 such molecules is set up using the simple square lattice packing. The head groups $-SiCl_3$ of the semi-fluorinated (SF) trichlorosilanes molecule $(CF_3(CF_2)_x(CH_2)_ySiCl_3$, with $x = 7$ and $y = 2$) are anchored to the Si substrate in Genzer and Efimenko's experiment, but constrained in our simulation with a harmonic potential ($k = 100$ kJ/mol/Å^2). The head group $-SiCl_3$ is also replaced by $-CH_3$ for simplicity (no force field parameters available for Si atom in OPLSAA force field[42]); we expect no significant changes in the water dynamics near the other side of the molecule due to the sufficiently

(31) Chau, C. L. *Mol. Phys.* **2003**, *101*, 3121−3128.
(32) Choudhury, N.; Pettitt, B. M. *Mol. Simul.* **2005**, *31*, 457−463.
(33) Choudhury, N.; Pettitt, B. M. *J. Am. Chem. Soc.* **2005**, *127*, 3556−3567.
(34) Choudhury, N.; Pettitt, B. M. *J. Phys. Chem. B* **2005**, *109*, 6422−6429.
(35) Vaitheeswaran, S.; Yin, H.; Rasaiah, J. C. *J. Phys. Chem. B* **2005**, *109*, 6629−6635.
(36) Sorin, E. J.; Rhee, Y. M.; Pande, V. S. *Biophys. J.* **2005**, *88*, 2516−2524.
(37) Wan, R.; Li, J.; Lu, H.; Fang, H. *J. Am. Chem. Soc.* **2005**, *127*, 7166−7170.
(38) Gao, J.; Qiao, S.; Whitesides, G. M. *J. Med. Chem.* **1995**, *38*, 2292−2301.
(39) Krafft, M. P.; Riess, J. G. *Biochimie* **1998**, *80*, 489−514.
(40) Lundgren, M.; Allen, N. L.; Cosgrove, T. *Langmuir* **2002**, *18*, 10462−10466.
(41) Reed, T. M. In *Fluorine Chemistry*; Simmons, J. H., Ed.; Academic Press: New York, 1964; Vol. 5, pp 133−221.
(42) Jorgensen, W. L.; Maxwell, D.; Tirado-Rives, J. *J. Am. Chem. Soc.* **1996**, *118*, 11225−11236.

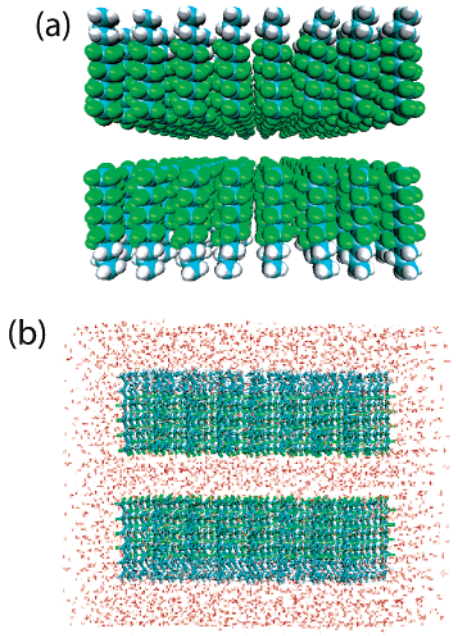

Figure 1. A scheme of the double fluorinated carbon plates system, with the $-CF_3$ groups of each surface facing each other (interplate distance $D = 8$ Å): (a) a perspective view of the double plates only; (b) an orthographic view of the solvated system. Each plate is made up of 64 superhydrophobic molecules aligned along the *z*-axis, which form an 8×8 regular square lattice on the $x-y$ plane.

long chain length. The 64 molecules are packed in such a way that they form an 8×8 regular square lattice parallel to the $x-y$ plane with the molecular axes aligned in the *z*-direction (see Figure 1). The optimal intermolecular spacing of fluorocarbons is found to be 5.7 Å, which is determined via energy minimization using the OPLSAA force field.[42] The double plates are made of two such layers separated by a variety of distances ranging from $D = 5$ to 15 Å, with the terminal $-CF_3$ groups facing each other (Figure 1 shows one example of the double plates at $D = 8$ Å). Both the single and the double plates are then solvated in water boxes, with water molecules at least 10 Å away from the solute surfaces (single plates solvated in the same $60 \times 60 \times 60$ Å^3 water box), with the total size of the solvated systems up to 25 000 atoms. The setup for the hydrogenated counterpart systems is basically the same, except that all fluorine atoms are replaced by hydrogen atoms and the optimal intermolecular spacing between successive hydrogenated molecules is now 4.8 Å. The smaller spacing of 4.8 Å in the hydrogenated system is due to the smaller hydrogen atoms as compared to fluorine atoms.

The GROMACS[43] program is used for the molecular dynamics simulations, with both the NPT (constant pressure and constant temperature, 1 atm and 300 K) and the NVE (constant energy and constant volume) ensembles for data collection. The OPLSAA force field[42] is adopted for the fluorinated solute molecules[44,45] and the SPC[46] model for the explicit solvent. The Particle Mesh Ewald (PME) method is used for the long-range electrostatic interactions, whereas a typical 10 Å cutoff is applied to the van der Waals interactions. The time step used for all molecular dynamics simulations is 1.0 fs. A standard conjugate gradient minimization is applied to relax the initial system. The minimized configurations are then used as the starting points for data collection of 2.0−3.0 ns for each system at 1 atm and 300 K. In most of the simulations, the positions of the fluorinated and hydrogenated molecules are restrained in space with a harmonic potential ($k = 100$ kJ/mol/Å^2 for the head group to mimic the "anchoring" to the substrate, and $k = 10$ kJ/mol/Å^2 for all other atoms), except when otherwise explicitly stated, such as in the kinetics simulations where the constraints in the *z*-direction are released to observe the hydrophobic collapse.

3. Results and Discussion

Before the production runs, we first performed some water contact angle calculations for the fluorinated carbon surface to compare with experiment as a validation of the OPLSAA force field and the SPC water model used in this study. Following a similar procedure used previously by Lundgren et al.[40] and Werder et al.,[47] we first prepared a water droplet of 900 water molecules with an initial rectangular shape, as shown in Figure 2a. The droplet was then introduced to the 8×8 fluorinated carbon molecule plate with a periodic box size of $60 \times 60 \times 65$ Å^3 (the box size is made sufficiently large to reduce the periodic image effect of water droplets). The system was equilibrated for 500 ps, and then 1.0 ns data (NVT ensemble at 300 K) were collected for production. During the simulation, the fluorocarbons were constrained with a harmonic potential ($k = 10$ kJ/mol/Å^2). A total of four independent simulations were run for data averaging starting from different initial configurations. The final results are insensitive to the initial configurations (we also tried initial spherical shapes, and results do not change). Figure 2b shows one representative snapshot at $t = 1$ ns. A common approach to extract the contact angle from nanoscale droplets is to fit the time-averaged liquid/vapor interface to a circle (see Figure 2c). Here, the liquid/vapor interface is defined as where the water number density falls to less than one-half that of the bulk (in practice, the droplet is divided into thin slices with a width of 1 Å parallel to the surface, and water number density is calculated for each bin[40,47]). By fitting the liquid/vapor profile to a circle, we obtained the water contact angle of $138 \pm 4°$, which agrees with the experimental value (up to 135°) very well. We have also calculated the water contact angle for its hydrogenated counterpart, and we found the angle to be $128 \pm 2°$. Indeed, the fluorinated carbon surface is more hydrophobic than its hydrogenated counterpart.

3.1. Hydration near a Single Fluorinated Surface. Hydration near Single Plates. The water density near a fluorinated superhydrophobic surface is expected to be somewhat lower than the bulk due to the "weak depletion" near the single surface. However, it is still of interest to see the strength of the water depletion near the fluorinated carbons as compared to the hydrogenated counterparts. Figure 3 shows the normalized water density profile as a function of the distance from the surface (*z*-axis) for both the fluorinated (red) and the hydrogenated (black) surfaces. The water density is normalized to 1.0 g/cm^3 at distances far from the surface. These density profiles are obtained by first equilibrating the systems with 1.0 ns simulations and then data collecting with the next 500 ps simulations with the NPT ensemble at 1 atm and 300 K. Each data point is averaged over a water layer 0.2 Å-thick in the *z*-direction and the same $x-y$ plane surface area as the plates. Clearly, the fluorinated surface has stronger water depletion than the hydrogenated surface. If we only count the water density within

(43) Lindahl, E.; Hess, B.; van der Spoel, D. *J. Mol. Mod.* **2001**, *7*, 306−317.
(44) Watkins, E. K.; Jorgensen, W. L. *J. Phys. Chem. A* **2001**, *105*, 4118−4125.
(45) Padua, A. H. *J. Phys. Chem. A* **2002**, *106*, 10116−10123.
(46) Berendsen, H. J. C.; Postma, J. P. M.; van Gunsteren, W. F.; Hermans, J. In *Intermolecular Forces*; Pullman, B., Ed.; Reidel: Dordrecht, 1981; pp 331−342.
(47) Werder, T.; Walther, J. H.; Jaffe, R. L.; Halicioglu, T.; Koumoutsakos, P. *J. Phys. Chem. B* **2003**, *107*, 1345−1352.

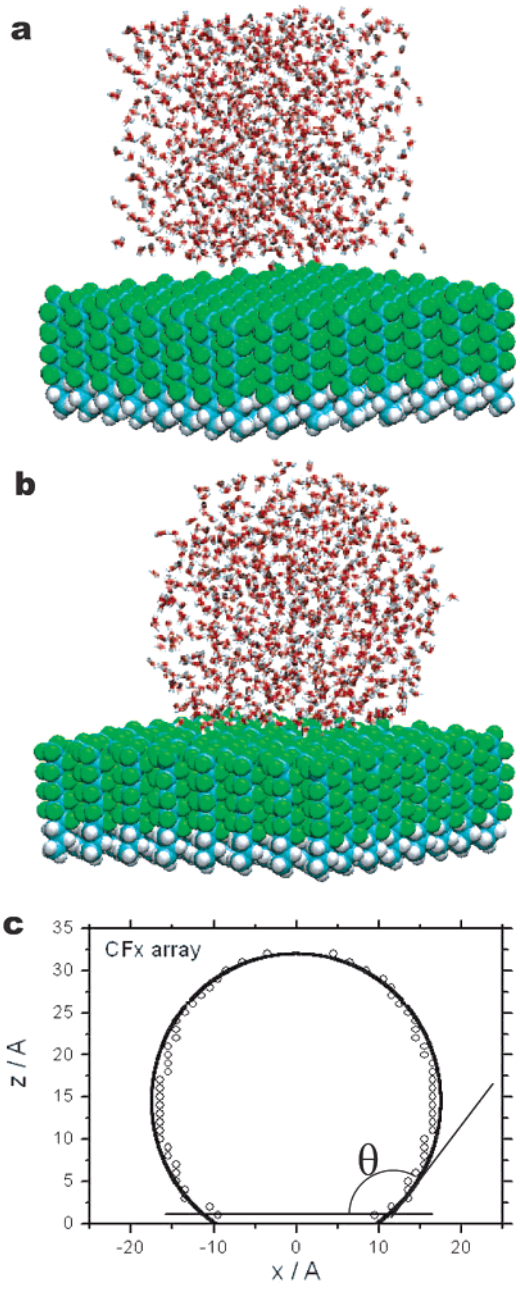

Figure 2. (a) Representative snapshot of the starting configuration at t = 0 ns for the water contact angle simulation on fluorinated carbon surface; (b) representative snapshot at t = 1 ns; (c) profile of the simulated water/vapor interface, fitted with a circle for the water contact angle calculation.

the first hydration shell of the single surfaces, the average water density (from the surface edge to the trough after the first peak around 4 Å in the density profiles) is approximately 0.67 g/cm^3 for the fluorinated surface and 0.72 g/cm^3 for the hydrogenated surface. If we include the water molecules in the second peak as well (from the surface edge to the trough after the second peak around 7 Å), the average water density becomes 0.78 g/cm^3 for the fluorinated surface and 0.83 g/cm^3 for the hydrogenated surface. Thus, the average water density close to the fluorinated superhydrophobic surface is about 6−8% lower than the hydrogenated counterpart. Interestingly, there are two recent experiments showing evidence for partial water depletion near paraffin-like hydrogenated carbon systems,[6−8] one by Steitz et al.[6] for D_2O in contact with deuterated polystyrene using neutron

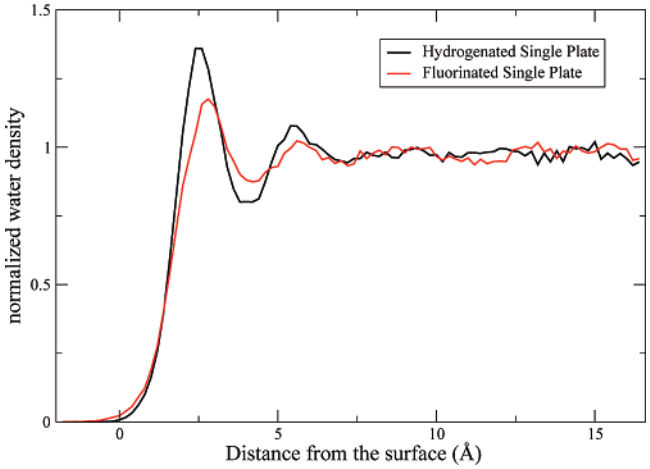

Figure 3. The profile of normalized water density as a function of distance from the surface for water near the single fluorinated plate (red) and hydrogenated plate (black). For the first and second solvation shells, the water density near the fluorinated plate is about 5−10% lower than that near the hydrogenated plate.

reflectivity experiment, and the other by Jensen et al.[7] with water in contact with paraffin using X-ray reflectivity experiment. These authors called the phenomena "partial dewetting", but basically it is nothing more than that the water density near the interface is somewhat (about 6−12%) lower than the bulk. Considering that their interface ranges (1−2 nm) are somewhat wider due to the experimental resolution limitations than our current ones in simulations (7−8 Å), our results for the hydrogenated carbons agree with experiment reasonably well. It is probably of interest to do similar X-ray or neutron reflectivity experiments for the fluorinated surfaces to verify this 6−8% extra lower water density in the partial-dewetting shell, as compared to the hydrogenated counterpart. It is also interesting to note that previous theories by Stillinger[13] and LCW[19] predict that for hard spheres there exists a vapor layer near the surface (for spheres with solute−solvent attractions, the drying interface is drawn closer to the hydrophobic surface due to the attraction[20]). Our current water density profile, however, shows a first-solvation peak (∼3 Å from the surface) near the superhydrophobic surface, which seems to contradict the previous theories. This peak in the water density profiles was also found in hydrophobic disks with weak solute−solvent attraction[29] and in solvated CF_4.[48]

Impermeability of Fluorocarbons. The experiment by Genzer and Efimenko[9] also indicated that the semi-fluorinated carbon molecules are impermeable; that is, water molecules are unable to penetrate through the fluorocarbons to stay inside the intermolecular spaces. To observe this impermeability in molecular detail, we "dig a hole" at the center of a single fluorinated plate by removing 2−4 fluorinated carbon molecules, thereby leaving sufficiently large space for water molecules to fill in the hole initially. It should be noted that the starting optimized "full plate" cannot contain any water molecules, because the intermolecular spacing of 5.7 Å is too small to host even a single water molecule. After removing 2, 3, and 4 fluorocarbon molecules, holes capable of filling 69, 78, and 96 water molecules (with bulk density) are created, respectively. We then carry out a 1.0 ns NVE simulation at 300 K to follow the

(48) Asthagiri, D.; Ashbaugh, H. S.; Piryatinski, A.; Pratt, L. R. LA-UR-06-3812, Los Alamos National Lab, 2006.

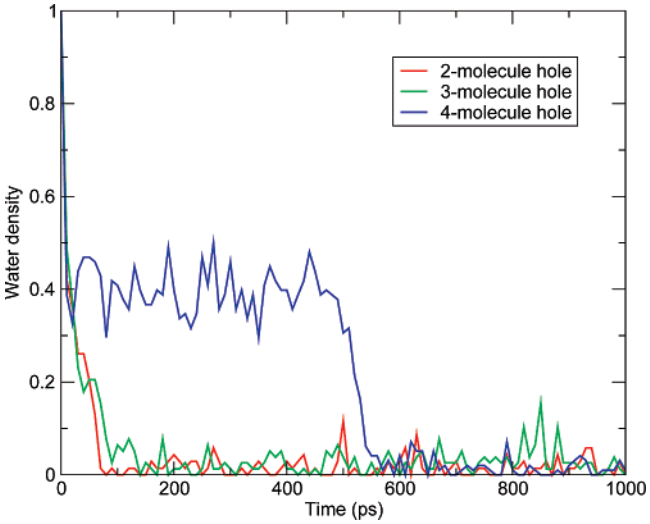

Figure 4. Illustration of the impermeability of the fluorinated carbon molecules. A "hole" near the center of the plate is created by removing 2−4 molecules from the plate lattice, which is then filled with water. A 1 ns MD simulation is performed on each solvated system to study the water permeability. It is shown that the water molecules inside the holes are gradually depleted, with the fluorinated molecules remaining impermeable thereafter.

trajectory of water molecules inside each hole. During the simulation, only the head groups of fluorocarbons are "anchored" (k = 100 kJ/mol/Å^2), but all of the other atoms are free to move. Figure 4 shows the water density inside the holes throughout the simulation for all three cases. It is found that these water molecules dissipate away into the bulk fairly quickly. In the cases of removing 2 and 3 fluorocarbon molecules, the water density decreases to zero within about 100−150 ps. In the case of removing 4 fluorocarbon molecules, the water density inside the hole reaches a moderate plateau of approximately 0.4 g/cm^3 (with about 40 water molecules trapped) in ∼50 ps and then remains there for about 400 ps (probably due to some kinetic trap, more trajectories are run and trapping happens in some trajectories but not all). The water density then starts to decrease again, with the hole completely depleted of water after 600 ps and remaining nonpermeable thereafter. These observations provide further evidence for the impermeable nature of fluorinated carbon monolayers as found by Genzer and Efimenko[9] in their experiment.

3.2. Dewetting in Fluorinated Double Plates. Dewetting Transition. It is of interest to see whether there is a dewetting transition in the superhydrophobic double plates when the plate−plate separation decreases to some threshold value. It is known from previous simulations[11,29,30] as well as macroscopic thermodynamic model that the critical distance for drying between the plates will increase as the strength of the attractive interaction decreases.[29] In general, it can be shown that when the water contact angle, θ_c, for water in contact with the hydrophobic plate is obtuse, the critical distance for dewetting $D_c \propto \cos\theta_c$.[29] The critical distance also increases linearly with the plate size when the plate is small.[29,30] Because the contact angle increases as the strength of the attraction between water and the plate decreases, the critical distance D_c should also increase (see eqs 5 and 9 in ref 29). As mentioned above, the water contact angle for paraffin is estimated to be about 115°[30] (the current hydrogenated counterpart is calculated to have a water contact angle of 128 ± 2°), which gives a critical distance of 6−8 Å

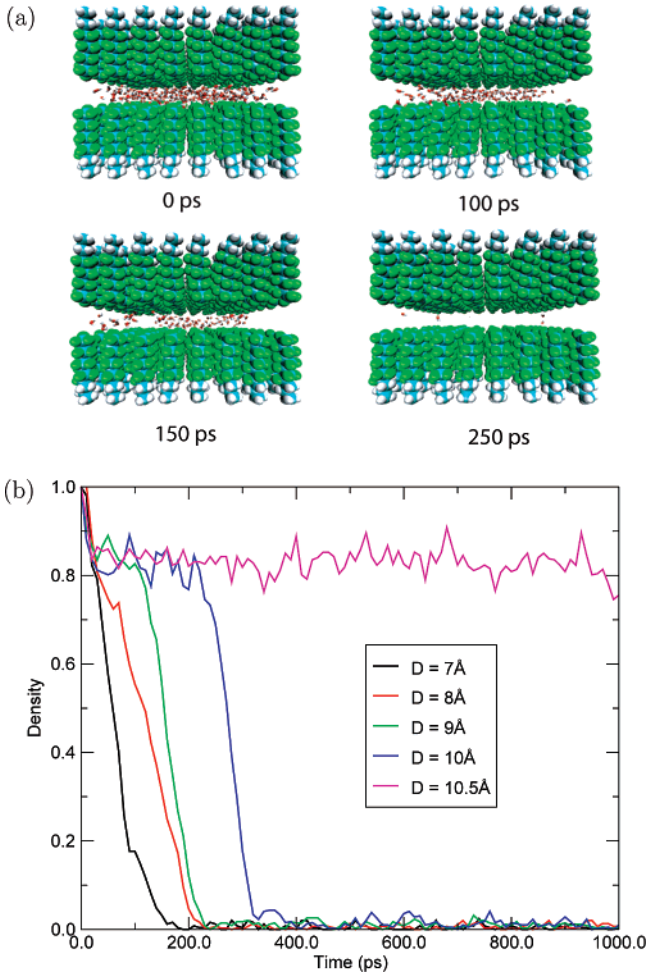

Figure 5. (a) The snapshots of the double fluorinated carbon plate system with D = 8 Å. Only water molecules within the interplate gap region are shown. It is clear that a sharp dewetting transition occurs within approximately 200 ps. (b) The trajectory of the water density inside the interplate region starting from various initial separation distances D for the fluorinated double plates.

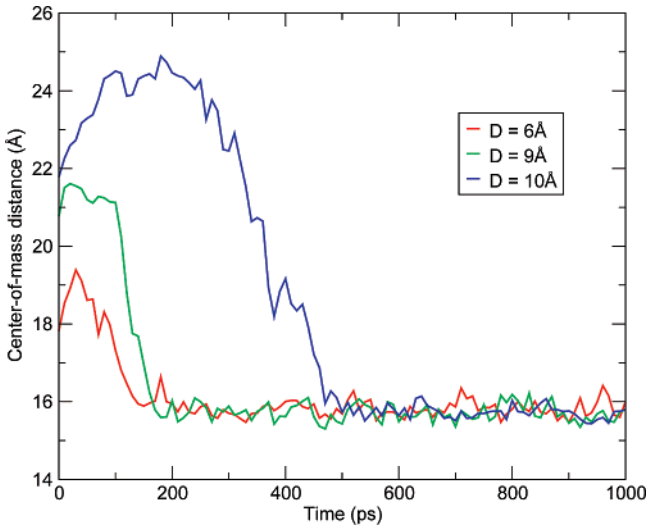

Figure 6. The center-of-mass distances of the two fluorinated plates versus time, as the two plates approach each other and collapse. Three different initial separations, D = 6, 9, and 10 Å, are shown in the figure.

according to the macroscopic theory (Figure 6 in ref 30). For the current fluorinated plates, a larger contact angle of 138 ± 4° was calculated (experimental value up to 135°). Together

with the larger molecular size (5.7 vs 4.8 Å in intermolecular separation), a larger critical distance is thus expected as compared to the paraffin-like plates or hydrogenated counterparts.

The simulation results confirm the above analysis based on the simple macroscopic thermodynamic theory.[29] Figure 5a displays a few snapshots of the double fluorinated carbon plate system with $D = 8$ Å. Only water molecules within the interplate gap region are shown for clarity. A sharp dewetting transition is observed after approximately 150−200 ps. Figure 5b shows the trajectories of the water density inside the interplate region starting from various initial separation distances for the fluorinated double plates. It is found that the water density inside the gap drops sharply within 400 ps for $D \leq 10$ Å, indicating a dewetting transition occurring in the gap region. The equilibrium water density inside the gap is essentially zero with only small positive bumps due to the presence of a few remaining water molecules lingering around the boundaries of the interplate region. In other words, for $D \leq 10$ Å, the vacuum state has a lower free energy than the liquid state for the interplate region. On the other hand, when the separation increases to above 10.5 Å, no such significant dewetting transition has been observed within 3.0 ns simulation at 1 atm and 300 K. This indicates a lower bound of the critical distance D_c of 10 Å for these fluorinated double plates. These findings are also confirmed by rewetting simulations, starting from initial dry conditions and looking for water molecules to rewet the region, indicating that the dry configurations are indeed thermodynamically more stable when the interplate distance D is less than 10 Å. Another interesting point to notice is that, although the time it takes to the initiation of the dewetting transition varies across different systems, the actual transition time after the initial diffusive motion is almost the same for all cases, about 100 ps! This is also consistent with previous findings with paraffin-like plates and idealized pure-hydrophobic plates.[29,30] It should be noted that we have also run simulations with other water models SPC/E[49] and TIP3P[50] to check the robustness of the current dewetting transition. The simulation results do not change much; a dewetting transition was observed in both SPC/E[49] and TIP3P[50] water models, with roughly the same dewetting critical distance around 10 Å (data not shown). Thus, the nanoscale dewetting transition seems fairly robust with regard to various water models.

Kinetics of the Hydrophobic Collapse. By relaxing the position restraints along the *z*-axis, we effectively allow the two plates to move relative to each other along the direction orthogonal to the surfaces. This is similar to the previous works on the hydrophobic dynamics of two paraffin-like plates or two-domain proteins,[11,30] where the two paraffin plates or two protein domains approach each other under the hydrophobic collapse forces. Again, a 3.0 ns NPT simulation is run for each system at 1 atm and 300 K for data collection. Here, we observe similar behavior for the superhydrophobic plates; that is, we find that the two surfaces are pushed together with a very fast speed, and meanwhile the water molecules in the interplate regions are depleted, as illustrated in Figure 6. The initial "bumps" in the curves (initial increases in the separations) are due to the fact that the plates are equilibrated with position restraints, so once the restraints are removed, the plates are pushed apart slightly in the beginning. Nevertheless, after the initial relatively slow diffusive motions, the two plates approach each other with a much faster speed (100−150 ps) as the water molecules are squeezed out of the interplate region. The liquid−vapor dewetting transition provides an enormous driving force toward further hydrophobic collapse for the double plates. When the initial interplate distance increases, it generally takes longer for the two plates to finally collapse (longer diffusive motions), reaching an equilibrium center-of-mass separation of 15−16 Å, with an average gap between two plates of only about 2−3 Å at the end. The reason we used the center-of-mass separation is because the fluorinated carbon chain molecules on both plates are not moving the same pace during the kinetics simulations, and it becomes ambiguous in defining a uniform plate-to-plate distance as we did for the above stationary plates; nevertheless, the overall picture for hydrophobic collapse stays the same.

Superhydrophobicity: Fluorinated versus Hydrogenated. In lieu of the above results for the dewetting transition in fluorinated double plates, a natural question arises: "Where does the dewetting transition stand for the hydrogenated counterparts?" In other words, what will the critical distance be for the hydrogenated double plates? Based on the above water contact angle argument as well as the smaller size (hydrocarbons are smaller than fluorocarbons), the critical distance should be smaller. Indeed, we are seeing a smaller critical distance for the hydrogenated counterpart plates. Figure 7a shows a similar dewetting behavior for the hydrogenated plates, but with a smaller critical distance of 8 Å. These results indicate that the drying transition becomes weaker in the hydrogenated plates as compared to the original fluorinated plates.

Now the question becomes: "What is the physical origin of the superhydrophobicity of these fluorinated plates, particularly given that fluorocarbons have much larger partial charges and dipoles (for example, with the OPLSAA force field, $q_C = 0.60$e, $q_F = -0.20$e in CF_3, whereas $q_C = -0.18$e and $q_H = 0.06$e in CH_3)?" Many previous studies have indicated that fluorinated chains can have significantly higher hydrophobicity than their hydrogenated counterparts, and some semiempirical rules, such as the well-known $1CF_2 \approx 1.5CH_2$ rule, have been proposed on the basis of the free energy of ligand partitioning and ligand binding;[38,39,51,52] however, the exact physical origin was not immediately clear. To further complicate the situation, there are also studies questioning the $CF_2 \approx 1.5CH_2$ rule from measurements of energies for adsorption and micellization of fluorinated amphiphiles.[53] One plausible explanation by Gao et al.,[38] based on their experiment on ligand partitioning and binding free energies, was that the stronger hydrophobicity of fluorocarbons was purely due to their larger surface area than hydrocarbons (ca. 30 vs 20 Å^2), which agrees with the $CF_2 \approx 1.5CH_2$ rule,[51,52] but again the explanation is more phenomenological than physical.

(49) Berendsen, H. J. C.; Grigera, J. R.; Straatsma, T. P. *J. Phys. Chem.* **1987**, *91*, 6269−6271.
(50) Jorgensen, W. L.; Chandrasekhar, J.; Madura, J. D.; Impey, R. W.; Klein, M. L. *J. Chem. Phys.* **1983**, *79*, 926−935.
(51) Shinoda, K.; Hato, M.; Hayashi, T. *J. Phys. Chem.* **1972**, *76*, 909−914.
(52) Mukerjee, P. *J. Am. Oil Chem. Soc.* **1982**, *59*, 573−578.
(53) Sadtler, V. M.; Giulieri, F.; Krafft, M. P.; Riess, J. G. *Chem.-Eur. J.* **1998**, *4*, 1952−1956.

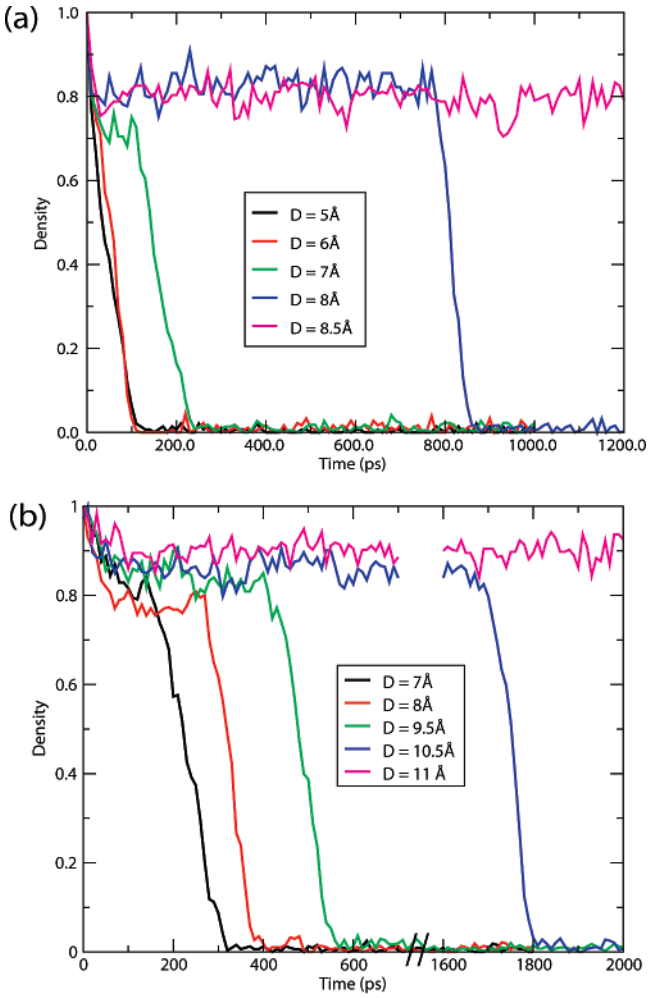

Figure 7. The trajectories of the water density inside the interplate region at various interplate distance D for the hydrogenated double plates with (a) the optimal intermolecular separation of 4.8 Å, and (b) an intermolecular separation of 5.7 Å, the same as that of the fluorinated molecules. It shows that the critical distance D_c increases from about 8 to about 10.5 Å when we enlarge the molecular separations from 4.8 to 5.7 Å.

To test the hypothesis of Gao et al.,[38] we can do some thought experiment by "adjusting" the intermolecular separation of hydrocarbons to mimic that of fluorocarbons. This can be easily achieved by replacing all of the F atoms in the fluorocarbons by H atoms and keeping their intermolecular separations of 5.7 Å "fixed" during the simulation (molecules constrained in their inflated positions by a stiff harmonic potential with a large $k =$ 100 kJ/mol/Å^2). If it is because of the larger surface area, then the "diluted" hydrocarbon system should show the same critical distance as the fluorocarbon plates. Indeed, the critical distance increases from 8 to about 10.5 Å, as shown in Figure 7b, reproducing the results of fluorocarbons. Both the "diluted" hydrocarbon−water interaction and the larger surface area contribute to this larger dewetting critical distance.

To further address the question on the physical origin of the superhydrophobicity for fluorocarbon plates, we calculate the interaction energy between water and plates for water molecules inside the gap region. Two double-plate systems, fluorocarbons with the intermolecular separation of 5.7 Å and hydrocarbons with the intermolecular separation of 4.8 Å, starting at the same interplate distance $D = 12$ Å, are used for this calculation. The 12 Å-thick interplate region is subdivided into 40 smaller layers with each 0.3 Å-thick for interaction energy profiling. Only the electrostatic and van der Waals (Lennard-Jones, in fact, but the $1/r^{12}$ term should not make much difference for our discussion due to its rapid decay) interactions between water molecules and plate solute molecules are collected; that is, no water−water or plate−plate interactions are included. A 500 ps NPT trajectory at 1 atm and 300 K is collected for each system for data averaging. Figure 8a shows the average water−plate interaction energy for the two systems (fluorocarbons, red; hydrocarbons, black). It is shown that water experiences a slightly weaker interaction, by up to 10−12%, from fluorinated plates than from the hydrogenated plates, in the nearest solvation shell (where the dewetting matters). This is somewhat counter intuitive, given that fluorocarbons have much larger partial charges, as mentioned above. Thus, we analyzed the interaction energy components, both the electrostatic and the Lennard-Jones energies, in detail. The results are shown in Figure 8b. Surprisingly, even though the electrostatic energies are indeed much stronger in the fluorocarbon plates than in the hydrocarbon plates (can differ by as much as a factor of 3 in near shells), the van der Waals energies dominate the water−plate interactions in near shells (with more than 90% contributions) and fluorocarbons have a noticeably weaker (by 10−15%) van der Waals interaction with water than do hydrocarbons. When the distance from the surface increases, the difference in both interactions gets smaller, and eventually the fluorocarbons can even show a slightly stronger interaction due to their larger partial charges (the electrostatic interactions decay slower than van der Waals). These results based on physical interactions provide a clearer view; both the slightly weaker water−plate interaction in near solvation shells and the larger surface areas contribute to the stronger dewetting transition in fluorocarbon plates. This weaker van der Waals interaction also makes sense, because fluorine is the most electronegative element and its dense electron cloud has very low polarizability.[39,41] This results in very strong intramolecular bonds and very weak intermolecular van der Waals interactions (also contributed by its relatively larger atomic size as compared to H atom; in essence, its larger size or surface area further "dilutes" its physical interactions with water). The very strong intramolecular bonds are responsible for the well-studied exceptional thermal and chemical stability; for example, fluorocarbons resist almost all corrosive environment, and no bacteria are known to feed on fluorocarbons. On the other hand, these very weak intermolecular van der Waals interactions with water are responsible for their unusual superhydrophobicity.

4. Conclusion

We have studied the hydration and dewetting near fluorinated carbon ($F(CF_2)_8(CH_2)_2SiH_3$) surfaces using molecular dynamics simulations. Our simulation results indicate that strong hydrophobicities are exhibited by these fluorinated molecular systems. A partial water depletion is found near the single fluorinated carbon surface, with an average water density in the first solvation shells 6−8% lower than its hydrogenated counterpart. The fluorinated molecules are also found to be water impermeable, consistent with the experimental findings. More remarkably, a sharp dewetting transition is found in the interplate region for the double fluorinated plates. This transition, although occurring on a microscopic length scale, is reminiscent of a first-order phase transition from liquid to vapor. By varying the

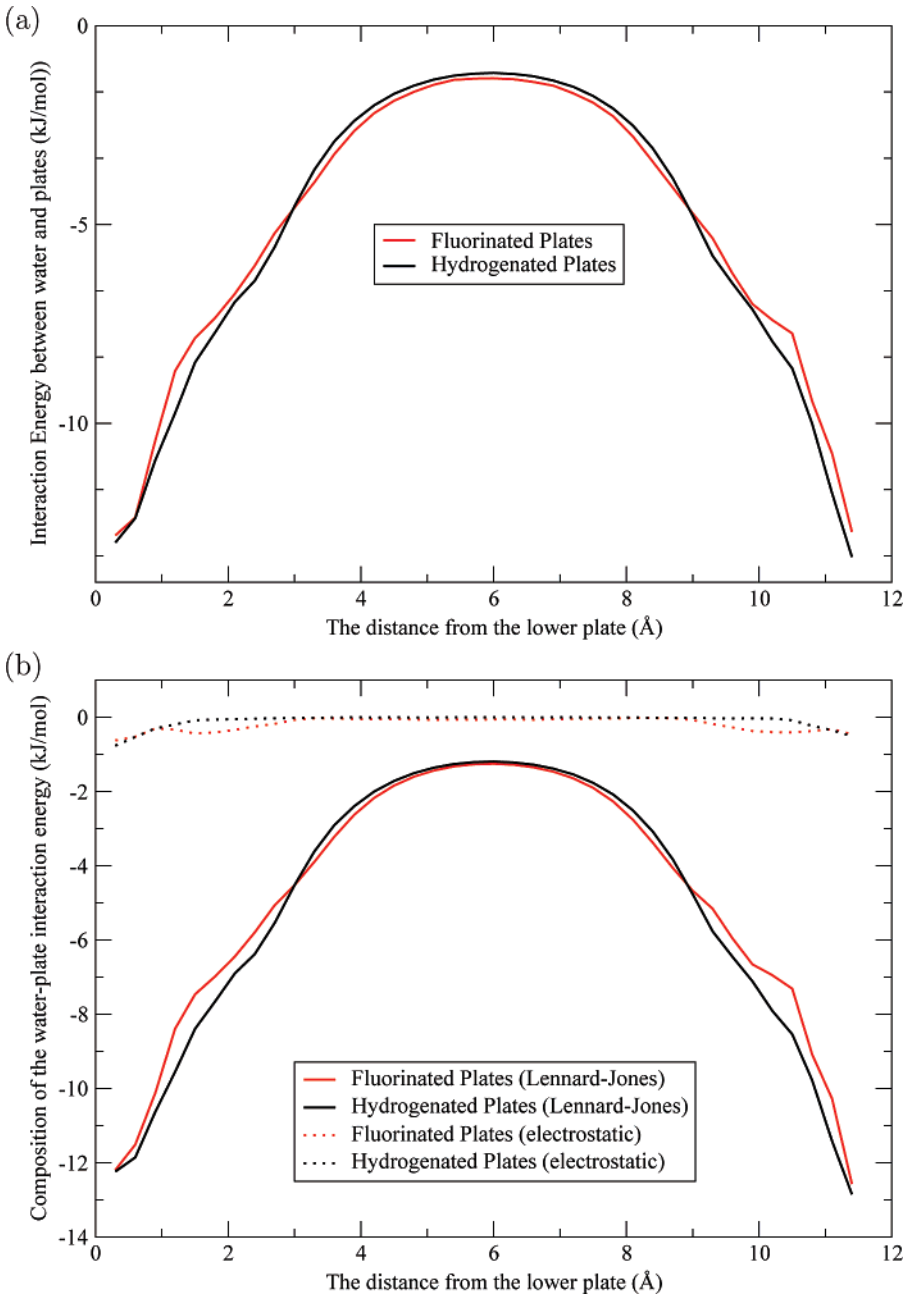

Figure 8. (a) The average interaction energy between water and double plates for water molecules inside the interplate region (fluorocarbons, red; hydrocarbons, black). The average interaction energies are obtained from averaging over a 500 ps trajectory and a water layer with a thickness of 0.3 Å and the same surface area as the double plates. (b) The detailed energy components, the electrostatic energy, and Lennard-Jones energy for the interaction energy profile in (a). It is clear that water experiences a similar interaction overall with both fluorinated and hydrogenated plates. The van der Waals energy dominates the water−plate interaction in both plates (see details in the text).

interplate distances, we find that dewetting occurs with a critical distance D_c up to 10 Å for an 8 × 8 double-plate system, upon which the interplate region is virtually vacuumed, with the exception of a few water molecules lingering around the boundaries of the interplate region. Such strong dewetting transition is remarkable as compared to its hydrogenated counterparts, as well as many other alternative systems, such as paraffin-like plates, which exhibit similar dewetting phenomena but with a smaller critical distance.

We have also made attempts to analyze the physical origin of this stronger dewetting transition and provided some evidence to explain the phenomena displayed by fluorinated carbons. The van der Waals interactions between water and plates are found to be the dominant force for the water−plate interaction as compared to the electrostatic interactions, and fluorocarbons show a 10−15% weaker van der Waals interaction with water than do hydrocarbons due to fluorine's low polarizability and relatively larger atomic size. In essence, the larger size or surface area "dilutes" fluorocarbons' physical interaction with water. Therefore, both the slightly weaker water−plate interaction in the nearest solvation shell and the larger surface area contribute to the stronger dewetting transition in fluorocarbon plates. Once the intermolecular separations of hydrocarbons are "inflated" to those of fluorocarbons to have the same surface area, the critical distance of hydrogenated plates approaches that of the fluorinated plates. These observations might help facilitate the

progress of molecular hydrophobicity studies and also have implications in a wide range of applications, such as submarine coating and novel water nanopore design.

Acknowledgment. We would like to thank Bruce Berne, Gerhard Hummer, Haiping Fang, Xuhui Huang, and Ajay Royyuru for many helpful discussions and comments. Part of the simulations were run on IBM BlueGene/L development machines, and we would like to thank Jose Castanos and his team for providing the running environment and Bob Walkup for help in porting the code to BlueGene/L.

JA057944E